

Conformations and dynamics of single flexible ring polymers in simple shear flow



Wenduo Chen ^{a, b}, Yunqi Li ^a, Hongchao Zhao ^c, Lijun Liu ^{b, *}, Jizhong Chen ^{b, *}, Lijia An ^b

^a Key Laboratory of Synthetic Rubber & Laboratory of Advanced Power Sources, Changchun Institute of Applied Chemistry, Chinese Academy of Sciences, 5625 Renmin Street, Changchun, 130022, PR China

^b State Key Laboratory of Polymer Physics and Chemistry, Changchun Institute of Applied Chemistry, Chinese Academy of Sciences, 5625 Renmin Street, Changchun, 130022, PR China

^c Changchun Institute of Optics, Fine Mechanics and Physics, Chinese Academy of Sciences, 3888 Dong Nanhu Road, Changchun, 130033, PR China

ARTICLE INFO

Article history:

Received 10 December 2014

Received in revised form

13 February 2015

Accepted 12 March 2015

Available online 19 March 2015

Keywords:

Ring polymers

Shear flow

Conformation

ABSTRACT

The conformational, orientational and dynamical properties of single flexible ring polymers under simple shear flow are studied by a hybrid multiparticle collision dynamics simulation method. We found that contributing to the continuous stretching and constant alignment in the tank-treading motion, ring polymers undergo weaker deformation and orientation in the gradient direction, and show similar behaviors in the vorticity direction compared with their linear analogues. We also present the mechanisms of both tumbling and tank-treading motions based on the time trajectories of relative deformation and orientation. Furthermore, the simulation results reveal that the special structures and unique dynamics of ring polymers in simple shear flow have an obvious influence on rheological properties, which are qualitatively different from the properties of linear polymers.

© 2015 Elsevier Ltd. All rights reserved.

1. Introduction

Ring polymers as one of the common forms have now been discovered in bacteria, plants and animals, such as plasmid, genome, actin, and polyose [1–5]. It is believed that the absence of end groups results in all monomers in a ring polymer are identical and the whole polymer prefers special conformations and dynamics [6]. This is not the case for linear polymers since the translational invariance along the chain is suddenly interrupted due to the terminal ends [1,7]. The rather extensive studies have been devoted to investigate the conformational and dynamical properties of linear polymers under shear flow [8,9], while the flow-induced behaviors of ring chains are still poorly understood. A deep insight into the basic conformational and dynamical properties of ring polymers in simple shear flow is highly needed in a wide range of biophysical fields, e.g. segregation of the cyclic genome from bacteria [4], migration of a cyclic DNA in a nanochannel [10] and ejection of viral DNA into the host [5].

The conformations as well as dynamics of individual linear polymers have been comprehensively understood in theories

[11–14], experiments [15–19] and simulations [20–24]. It is a well-known fact dating back to 1974 that De Gennes described the coil-stretch transition of linear polymer chains in shear flow [11]. The theory predicted that when a certain critical value of the velocity gradient is reached, the fluid viscous forces are greater than the entropic elastic retraction forces and the chain is stretching. Traditional experiments involving optical techniques such as birefringence and light and neutron scattering have sought average structural information of linear polymers in shear flow [25,26]. Chu and his co-workers have shed light on the conformations and dynamics of an individual DNA via fluorescence microscopy [17,27,28]. They observed directly that DNA molecules indeed substantially stretch and continually undergo end-over-end tumbling motion as reflected in large conformational fluctuations. More recently, Steinberg groups studied the orientation angles of λ -DNA relative to the shear plane by particle image velocimetry measurements [19]. They found that the strong deviation of the probability distribution functions of the orientation angles from Gaussian distribution is in good accord with theory. Besides experiment and theory, Larson et al. studied the deformations and tumbling dynamics of individual polymer chains in shear flow via Brownian dynamics (BD) simulations [23,29]. They found that the decrease in chain stretch ceases at sufficiently large flow shears. Furthermore,

* Corresponding authors.

E-mail addresses: ljlui@ciac.ac.cn (L. Liu), jzchen@ciac.ac.cn (J. Chen).

the knowledge of the flow-induced conformational information can be used to calculate rheological properties such as shear viscosity [30,31]. Doyle et al. used BD to simulate rheological properties by conformational properties such as shear viscosity and normal stress differences [31].

The flow-induced behaviors of ring polymers are generally related to separation required for identification, quantification, purification, and fractionation [32–36]. Zheng and Yeung separated circular ϕ X174 RF DNA from λ DNA, based on their radial migration in capillary electrophoresis with applied hydrodynamic flow [36]. Cramail and his coworkers purified the synthesis macrocyclic polystyrenes from the residual linear precursor and byproducts by liquid chromatography [34]. Although the flow-induced behaviors are very important in separation processes, the conformations as well as dynamics of single flexible ring polymers in shear flow have still remained elusive. Cifre et al. studied the stretching behaviors of ring polymers in simple shear flow by BD simulation and demonstrated that the shear dependence of the average extension of ring polymers is analogous to that of linear polymers [37]. Recently, our groups studied the dynamics of individual ring polymers in simple shear flow by the multiparticle collision dynamics (MPCD) method [38,39]. The results revealed that individual ring polymers exhibit two primary types of motion, continually end-to-end tumbling like linear polymers and tank-treading like fluid droplets and capsules. Frey and his co-workers also found the two types of motion and used the time evolution of the orientation angle to distinguish these motions [40]. Though various novel behaviors of ring polymer in shear flow have been revealed, qualitative and quantitative studies on how the conformation and orientation of single flexible polymer chains response to shear flow are still far from clear.

Computer simulation plays an important role in studying instantaneous dynamics of a single polymer in shear flow since simulation can provide a bridge between theory and experimental observation [41,42]. In this work, we present the detailed simulation results of the conformational, dynamical, and rheological properties of single flexible ring polymers in steady shear flow. We apply a hybrid simulation approach, combined MPCD method describing the solvent with molecular dynamics simulation (MD) for the polymers [43,44]. As has been shown, the MPCD method has the virtue of taking into account hydrodynamic interactions and thermal fluctuations, which is suited to study the non-equilibrium properties of polymers under shear flow [45–50].

The outline of the paper is as follows: In Section 2, we describe the model and simulation approach. In Section 3, the conformational and orientational properties of flexible ring polymers under simple shear flow are presented. Then a deep research is given for tumbling and tank-treading motions. We also discuss the contribution of ring polymers to the rheological properties. In Section 3.3, we generalize our studies and give a conclusion.

2. Model and simulation method

In our model system, flexible ring polymer chains consist of N_{se} beads of mass M each [51,52], which are connected by the finitely extensible nonlinear elastic (FENE) potential U_{FENE} ,

$$U_{FENE}(r) = \begin{cases} -\frac{1}{2}KR_0^2 \ln \left[1 - \left(\frac{r}{R_0} \right)^2 \right] & r \leq R_0 \\ \infty & r > R_0 \end{cases} \quad (1)$$

where R_0 is the maximum bond length and K is the spring constant.

The excluded-volume interactions between beads are taken into account by a truncated and shifted Lennard-Jones potential U_{LJ} :

$$U_{LJ} = \begin{cases} 4\epsilon \left[\left(\frac{\sigma}{r} \right)^{12} - \left(\frac{\sigma}{r} \right)^6 \right] + \epsilon & r \leq r_{cut} \\ 0 & r > r_{cut} \end{cases} \quad (2)$$

where $r = |\mathbf{r}_i - \mathbf{r}_j|$ denotes the spatial distance between beads i and j located at \mathbf{r}_i and \mathbf{r}_j . The parameters ϵ and σ are taken as the units of energy and length, respectively. The short-range, purely repulsive interactions are taken into account by choosing $r_{cut} = 2^{1/6}\sigma$. The velocity Verlet algorithm with time step h_p is used to integrate Newton's equations of motion of beads.

The explicit solvents are simulated by the MPCD method, which consists of streaming and collision steps [43,44]. Solvents are modeled as N_{st} point-like particles of mass m . In the streaming step, the solvent particles propagate ballistically and their positions are updated according to [53].

$$\mathbf{r}_i(t+h) = \mathbf{r}_i(t) + h\mathbf{v}_i(t) \quad (3)$$

where $i = 1, \dots, N_{st}$ and the collision time h is the time interval between collisions. In the collision step, the particles are sorted into cubic cells with length a , and their relative velocities, with respect to the center-of-mass velocity of each cell $\mathbf{v}_{cm}(t)$, are rotated by an angle α around a random axis $\mathbf{R}(\alpha)$ [43], i.e.

$$\mathbf{v}_i(t+h) = \mathbf{v}_{cm}(t) + \mathbf{R}(\alpha)[\mathbf{v}_i(t) - \mathbf{v}_{cm}(t)] \quad (4)$$

where $\mathbf{v}_i(t)$ is the velocity of particle i at time t and the center-of-mass velocity

$$\mathbf{v}_{cm}(t) = \frac{1}{N_{st}^c} \sum_{j=1}^{N_{st}^c} \mathbf{v}_j(t) \quad (5)$$

N_{st}^c is the total number of solvent particles within the collision cell.

The solute-solvent coupling is achieved by taking the solute into account in the collision step, and velocities of the center-of-mass are [43,44].

$$\mathbf{v}_{cm} = \frac{\sum_{i=1}^{N_{st}^c} m\mathbf{v}_i(t) + \sum_{j=1}^{N_{se}} M\mathbf{v}_j(t)}{mN_{st}^c + MN_{se}} \quad (6)$$

where N_{se}^c denotes the number of monomers in the cell. Mass, momentum, and energy are conserved in the collision step. In addition, a random shift is performed to ensure Galilean invariance at every collision step [54].

Lees–Edwards boundary conditions are applied for the solvent particles and the solute beads in order to impose shear flow [55]. The velocity field is given by

$$v_x = \dot{\gamma}y, \quad v_y = 0, \quad v_z = 0 \quad (7)$$

The schematic representation of a flexible ring polymer in simple shear flow is shown in Fig. 1. A local Maxwellian thermostat is used to maintain the temperature of the system at the desired value [56].

All simulations are performed with the rotation angle $\alpha = 130^\circ$, $\sigma = 1.0$, $a = \sigma$, $\epsilon = 1.0$, $k_B T/\epsilon = 1$, where T is the temperature and k_B is the Boltzmann constant. The collision time $h = 0.1\tau_p$, MD time step $h_p = 0.005\tau_p$, with $\tau_p = \sqrt{ma^2/(k_B T)}$. Small collision time h and large rotation angle α are used to obtain large Schmidt numbers required for fluid-like behaviors [53,57]. The average number of solvent particles per collision cell $\rho = 10$, and $M = \rho m$. The maximum bond length $R_0 = 1.5\sigma$ and the spring constant $K = 30\epsilon/\sigma^2$. The viscosity of solvent fluid [58] is $8.7(\epsilon m)^{1/2}/\sigma^2$. The chain

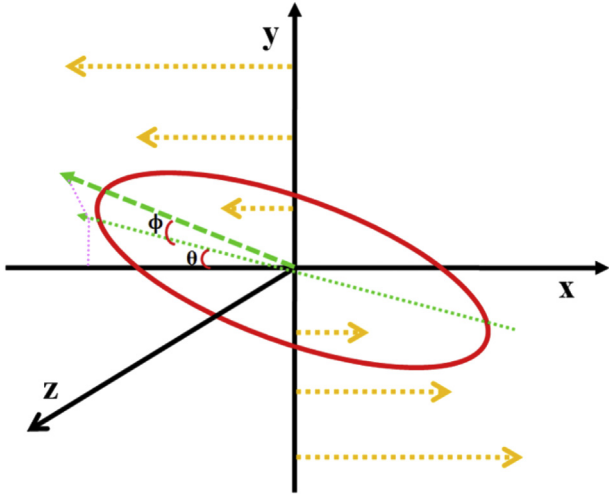


Fig. 1. Sketch of a single ring polymer in simple shear flow. ϕ is the angle between the principal vector and its projection onto the flow-gradient plane and θ is the angle between this projection and the flow direction.

lengths range from 40 to 200, and accordingly system sizes from $40a \times 20a \times 20a$ to $150a \times 40a \times 40a$.

3. Results and discussion

Now we will discuss the flow-induced properties of single ring polymers in simple shear flow. The strength of the applied shear flow is characterized by the dimensionless Weissenberg number $Wi = \dot{\gamma}\tau$, where $\dot{\gamma}$ is shear rate and τ is the longest equilibrium relaxation time [59]. In the small shear regime ($Wi < 1$), the conformations of the polymer coils have no detectable changes respect to the equilibrium conformation. However, in the strong shear regime ($Wi > 1$), the ring chains have strong deformations and orient with the flow direction. The characteristic value $Wi = 1$ plays an essential role in characterizing the microscopic conformational and orientational properties of individual chains in simple shear flow [13,27].

3.1. Conformational properties

A convenient quantity to characterize the conformational properties of polymer chains in shear flow is the gyration tensor $G_{\alpha\xi}[\alpha, \xi \in (x, y, z)]$ [52]. The average gyration tensor $\langle G_{\alpha\xi} \rangle$ is directly accessible in light scattering and fluorescence microscopy experiments [17,25,62]. The diagonal components $\langle G_{\alpha\alpha} \rangle$ are the squared radius of gyration. In the absence of flow, the statistical conformation of ring polymers is spherical, thus, $\langle G_{xx} \rangle = \langle G_{yy} \rangle = \langle G_{zz} \rangle = \langle R_{g0}^2 \rangle / 3$ (R_{g0}^2 is the mean-square radius of gyration at equilibrium state). The three eigenvalues of $G_{\alpha\xi}$ are denoted by the largest eigenvalue G_1 , the middle G_2 and the smallest G_3 , and their sum is just R_g^2 [55]. They can fully satisfy identifying the deformation of ring polymers under shear flow.

Fig. 2 displays three diagonal elements of the gyration tensor $\langle G_{\alpha\xi} \rangle$ at steady state scaled with R_{g0}^2 as a function of Wi with various lengths. The mean polymer extensions in simple shear flow are described by the flow component of the gyration tensor $\langle G_{xx} \rangle$. As shown in **Fig. 2(a)**, for $Wi < 1$, $\langle G_{xx} \rangle$ are only weakly perturbed. In this regime, ring polymers have no obvious deformation and only align along the flow direction. It is worth noticing that the relative stretching $3\langle G_{xx} \rangle / R_{g0}^2$ is essentially independent of chain length and the data of different lengths collapse onto a universal curve. The deformation ratios $3\langle G_{xx} \rangle / R_{g0}^2 - 1$ exhibit a Wi^2 power law

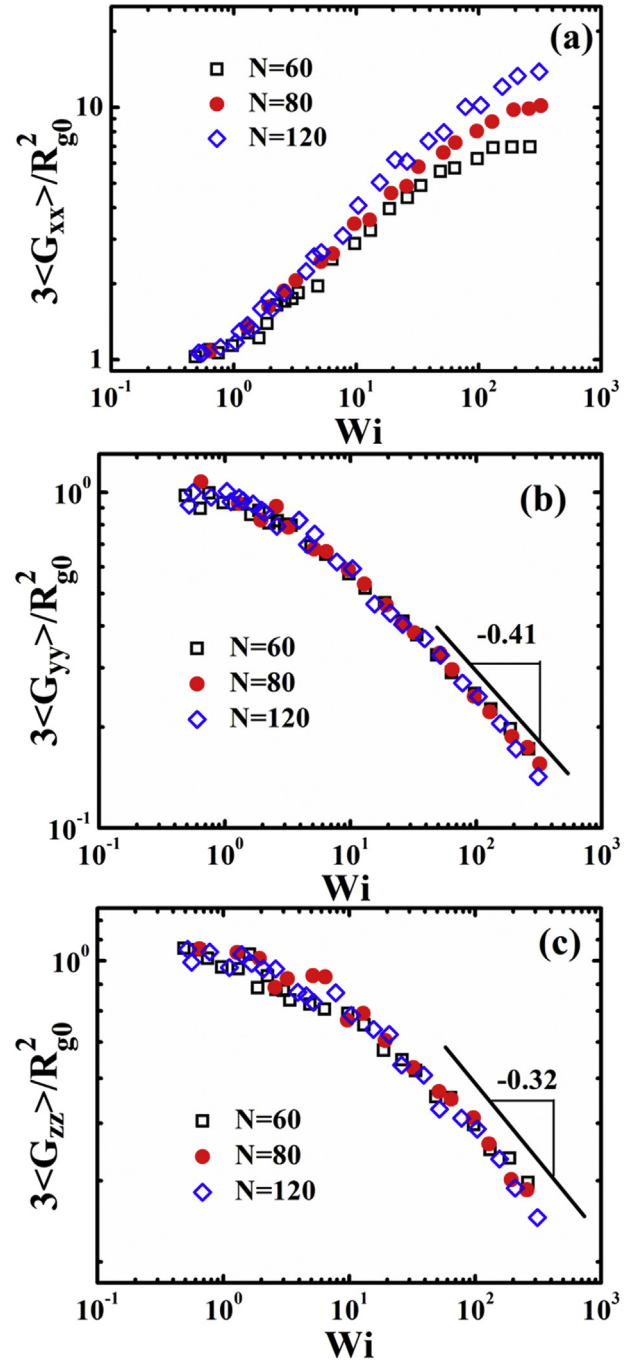


Fig. 2. (a) The flow component of the gyration tensor $\langle G_{xx} \rangle$, (b) the gradient component $\langle G_{yy} \rangle$, and (c) the vorticity component $\langle G_{zz} \rangle$ as a function of the Weissenberg number Wi for ring polymers with various chain lengths. R_{g0}^2 is the gyration tensor at equilibrium.

dependence [38], which is consistent with the theoretical and numerical studies for single linear polymers in a dilute solution [13,60]. With Wi increases, the values of $\langle G_{xx} \rangle$ increase rapidly, implying that ring molecules not only orient with the flow direction but also assume a stretched conformation. At high Weissenberg numbers ($Wi > 20$), a platform appears as a consequence of the finite chain extensibility which yields an average extension smaller than half of the contour length [13,61]. Furthermore, the stretching of various polymer lengths achieves the different asymptotic values. It reflects the fact that the maximum extension dependent

on the finite size of ring polymers. Furthermore, we compared the extension of ring polymers with linear polymers of the same molecular weight. The results show that the ring polymers are obviously less deformed than the linear ones. A similar stretching behavior was also observed by Cifre et al. using BD simulations [37].

The ensemble-averaged gradient component of the gyration tensor $\langle G_{yy} \rangle$ is tightly linked with the mean thickness of polymers that has direct influence on the polymer contribution to the shear thinning of a dilute solution [27]. When shear rates are small ($Wi < 1$), the value of $3\langle G_{yy} \rangle / R_{g0}^2$ is about 1, reflecting the fact that the deformation is undetectable. With Wi increases, the extension of ring polymers in the flow direction are accompanied by shrinking in the gradient and vorticity directions. Different from the flow component, the values of $\langle G_{yy} \rangle / R_{g0}^2$, for a given Wi , are practically independent of chain length, and a universal power law $\langle G_{yy} \rangle / R_{g0}^2 \sim Wi^{-0.41}$ is obtained over the considered Wi range ($Wi > 20$), as shown in Fig. 2(b). Interestingly, the scaling exponent -0.41 obtained here is larger than -0.50 for the flexible linear polymers in previous experiments and simulations [27,62]. The slow decays of $\langle G_{yy} \rangle$ is attributed to the continuous stretching along the flow direction and constant compression in gradient direction in tank-treading motion.

Fig. 2(c) presents the ensemble-averaged vorticity component of the gyration tensor $3\langle G_{zz} \rangle / R_{g0}^2$. With increasing Wi , the values of $\langle G_{zz} \rangle$ drop significantly from a plateau value. The slopes of the curves for ring polymers with different lengths predict a universal dependence, $\langle G_{zz} \rangle / R_{g0}^2 \sim Wi^{-0.32}$. The result is similar to the scaling $Wi^{-0.34}$ established previously for the flexible linear polymers [27,62]. It implies that the tank-treading motion has no obvious influence on the compression in vorticity direction.

The three eigenvalues of $G_{\alpha\zeta}$ give the principal axes of polymer chains. The ratio G_1/G_3 denotes the asphericity of polymer chains because if the value of G_1/G_3 does not equal to unity means that the distribution is nonspherical, while it diverges in the limit of a long rod [55]. In order to gain a deeper understanding of the deformation of ring polymers under simple shear flow, the ratio $G_1/G_3 - 1$ as a function of Wi for various chain lengths is shown in Fig. 3. The changes of shape are independent of the chain length for all of the simulation points almost falling on the same straight line. At small Weissenberg numbers ($Wi < 1$), we find that $G_1/G_3 - 1$ is independent of Wi , implying that the chains are close to their equilibrium structure and only align along the flow direction. With increasing Wi , single ring polymers have obvious deformations corresponding to the increasing of the ratios. At large Weissenberg

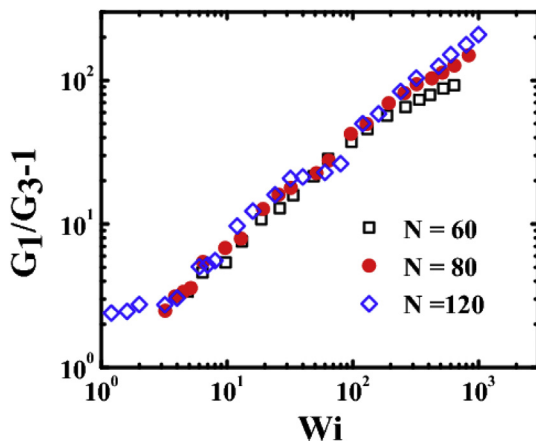


Fig. 3. Ratio of the largest (G_1) and smallest (G_3) eigenvalues of the average gyration tensor as a function of the Weissenberg number Wi with various chain lengths.

numbers ($Wi \gg 1$), a chain-length dependence appears associated with the finite size of ring polymers.

3.2. Orientational properties

The flow-induced alignment of flexible ring polymers is quantified by the angle θ , which is the angle between the eigenvector of the gyration tensor with the largest eigenvalue and the flow direction [see Fig. 1], straightforwardly obtained from the components of the radius of gyration tensor via [13,39].

$$\langle \tan(2\theta) \rangle = \frac{2\langle G_{xy} \rangle}{\langle G_{xx} \rangle - \langle G_{yy} \rangle} \quad (8)$$

It is noticed that the average deformation and orientation can be directly accessed in light scattering [25], neutron scattering [63] and birefringence [64–66] experiments. Recently, fluorescence microscopy allows for direct observation of DNA molecules in single molecule experiments [17].

A universal curve is obtained for the average orientation angle $\langle \tan(2\theta) \rangle$ with various lengths as a function of Wi . At small shear ($Wi < 1$), G_{xy} is proportional to Wi and $G_{xx} - G_{yy}$ is proportional to Wi^2 . Hence, $\langle \tan(2\theta) \rangle$ decreases linearly as the shear rate increases, as shown in Fig. 4. With increasing Wi , the ring chains become not only stretched but also more closely aligned with the flow direction. In the strong flow regime ($Wi > 20$), the orientation angle decays and a new scaling regime appears, where $\langle \tan(2\theta) \rangle \sim Wi^{-0.40}$. This scaling is larger than the exponent found for linear polymers exhibiting only tumbling motion -0.46 [27]. Clearly, the special dynamics make the scaling behavior of the orientation of ring polymers different from linear chains. This can be attributed to the fact that a single ring adopts a continuous elliptical shape and maintains a constant orientation angle in the flow-gradient plane for tank-treading motion [38].

In order to give a further insight into the orientational behavior of ring polymers, the probability distribution functions (PDFs) $P(\theta)$ are calculated. At equilibrium, no angle is preferred and $P(\theta)$ is uniform PDF, whereas an increasing Wi leads to the appearance of a peak and the PDF maximum is located at positive value, as shown in Fig. 5(a). As shear rate increases, the peak shifts to the smaller values, at the same time, the width of $P(\theta)$ decreases. An apparent shift of the data is explained that ring polymers are strongly deformed and aligned with the shear flow. Furthermore, $P(\theta)$ can be described by a power law $P(\theta) \sim (\sin\theta)^{-2}$ in the limit of sufficiently large shear, which is in accord with the depiction for linear

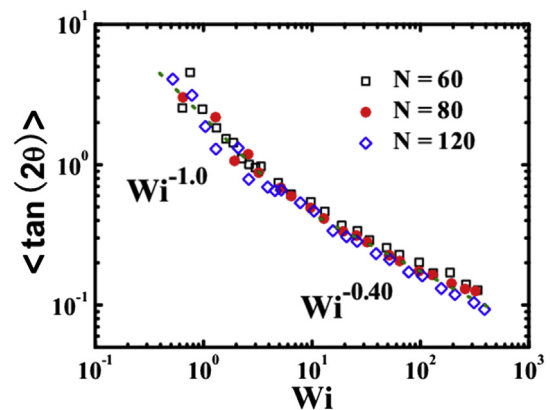


Fig. 4. Orientation angle $\langle \tan(2\theta) \rangle$ as a function of the Weissenberg number for ring polymers with several lengths. The dashed lines represent the dependences $\langle \tan(2\theta) \rangle \sim Wi^{-1.0}$ for ($Wi < 1$) and $\langle \tan(2\theta) \rangle \sim Wi^{-0.40}$ for ($Wi > 1$).

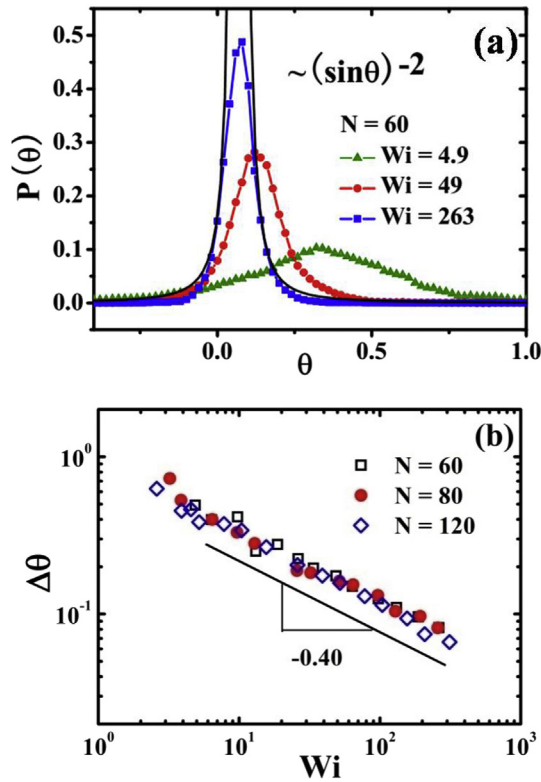


Fig. 5. (a) Probability distribution functions $P(\theta)$ in log coordinates with chain length $N = 60$. The solid line presents the theoretical prediction $(\sin\theta)^{-2}$. (b) The widths at half height $\Delta\theta$ as a function of Weissenberg number. The solid line indicates the power law $\Delta\theta \sim Wi^{-0.40}$.

polymers [67,68]. Fig. 5(b) displays the half-height width of $P(\theta)$ as a function of Weissenberg number with different chain lengths. $P(\theta)$ follows power-law decays according to $\Delta\theta \sim Wi^{-0.40}$, different from theoretical and experimental predictions for linear polymers $\Delta\theta \sim Wi^{-0.51}$ [13]. This can be explained by the fact that ring polymers adopt the constant positive orientation in tank-treading motion [38].

To fully characterize the orientational properties relative to the shear flow, the probability distribution functions $P(\phi)$ are measured, where ϕ is the angle between the principal vector and its projection onto the flow-gradient plane, as shown in Fig. 1. Fig. 6(a) displays $P(\phi)$ of flexible ring polymers as a function of Wi with various chain lengths. With increasing Wi , $P(\phi)$ undergo a crossover from a Gaussian shape of the distribution function to a power-law decay, which is also observed for linear polymers [67,68]. The PDF tails for all values of Wi decay algebraically with the exponent rather close to the theoretical ϕ^{-2} for linear polymers. For flexible ring polymers, we obtain a universal exponent for $Wi \gg 1$. As shown in Fig. 6(b), the half-height width $\Delta\phi$ decreases as $Wi^{-0.41}$, slightly less than $Wi^{-0.38}$ for linear polymers [13]. It implies that the tank-treading motion have weak influences on the off-plane orientation.

3.3. Tumbling and tank-treading motions

In this section we present the mechanisms of both tumbling and tank-treading motions for ring polymers. The geometrical constraint of ring polymers leads to the unique dynamics as well as the intricate conformational properties in simple shear flow [38,39]. In order to directly observe the dynamics of single rings, we show trajectories of polymer extension and orientation angle. The

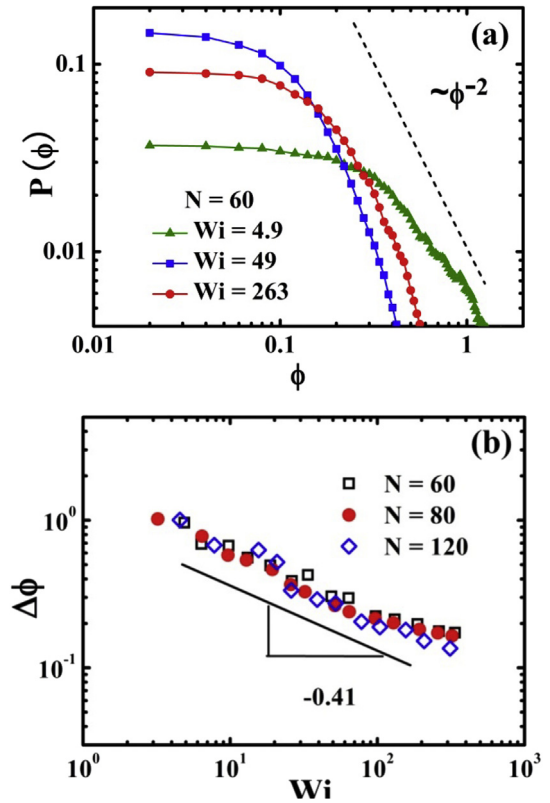


Fig. 6. (a) Probability distribution functions $P(\phi)$ with chain length $N = 60$. The dashed line presents the theoretical prediction ϕ^{-2} . (b) The widths at half height $\Delta\phi$ as a function of Weissenberg number. The solid line indicates the power law $\Delta\phi \sim Wi^{-0.41}$.

time traces of the orientation angle θ and the associated distortions of polymer coils from equilibrium $G_{xx}/\langle G_{xx} \rangle - 1$ are shown in Fig. 7. When rings undergo tank-treading motion in regime I, polymer assumes a constant inclination angle with small fluctuations and the continuous extension G_{xx} is much larger than the statistic values under shear $\langle G_{xx} \rangle$ [38]. When ring polymers tumble in regime III, ring chains continually undergo stretching, aligning, flipping, and collapsing phases of end-over-end tumbling motion. Besides these two regions, there is a mixture region, regime II, having characters of both tank-treading and tumbling regions.

We propose the following general description of the tank-treading and tumbling mechanisms in strong shear flow ($Wi > 1$)

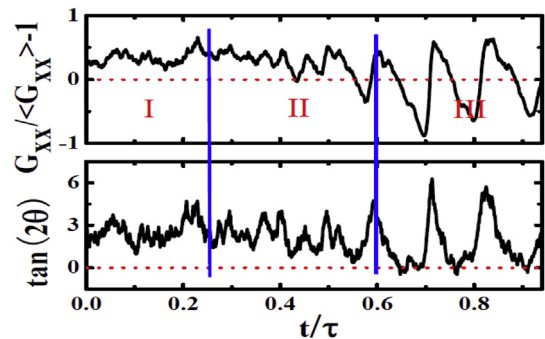


Fig. 7. Time trajectories of the relative deformation $G_{xx}/\langle G_{xx} \rangle - 1$ and orientation $\tan(2\theta)$ for a single flexible ring with chain length $N = 40$ at $Wi = 510$ in simple shear flow, where $\langle G_{xx} \rangle$ is the mean extension. A tank-treading motion in regime I, a tumbling motion in regime III, and a crossover from tank-treading motion to tumbling motion in regime II.

based on the time sequence of images of the dynamical behaviors for single ring polymers. In tumbling motion, the ring chain collapses rapidly and tumbles with large deformations, which is well-known for linear polymers under shear [17]. As shown in Fig. 8(a), the shear gradient across the single ring leads to polymer stretching and the orientation angle is positive ($\theta > 0$). After stretching, a ring polymer generally aligns with the flow direction ($\theta \approx 0$) with $G_{xx} > \langle G_{xx} \rangle$, leading to the small velocity differences across the chain, and, the thermal disturbance leads orientation angle to become negative ($\theta < 0$). Then, the ring polymers collapse with highly negative values ($\theta \ll 0$). Finally, the polymer tumbles to avoid large shear gradient, and the orientation angle changes sign from negative to positive.

In tank-treading motion, the chain adopts an elliptical shape in the flow-gradient plane due to the strong excluded volume interactions between the two strands of flexible ring polymers. The monomers move around the center of mass of a single chain within the xy -plane, which is similar to red blood cells [69,70]. During this progress, the individual ring polymer adopts a constant extension and orients with a positive orientation angle. When the plane of the stretched rings coincides with the shear plane, a substantial velocity gradient along the contour causes the ring chains to perform a tank-treading motion, and the torque balance leads to a non-vanishing angular velocity [see Fig. 8(b)]. Since the force due to the shear flow lacks a component to change the orientation of the ring plane, a ring prefers a constant inclination angle with small fluctuations [40]. For highly inherent deformability of the flexible ring polymers, the stability of pure tank-treading motion is relatively poor. The strong thermal fluctuation causes instability of the elliptical shape in the flow-gradient plane and results in the termination of tank-treading motion and the initiation of tumbling motion.

3.4. Rheological properties

The shear viscosity and the first normal stress difference as two major properties of dilute polymer solutions have been identified in experiment, theory and simulation. In the dilute solutions, the macroscopic rheological properties can be calculated though the microscopic conformational information on polymer chains. The effect of the dissolved polymers on the solution viscosity is resolved by studying the intrinsic stress tensor [37,71].

$$\tau_{\alpha,\beta} = \sum_{i=1}^N \langle \mathbf{R}_{i,\alpha} \cdot \mathbf{f}_{i,\beta} \rangle \quad (9)$$

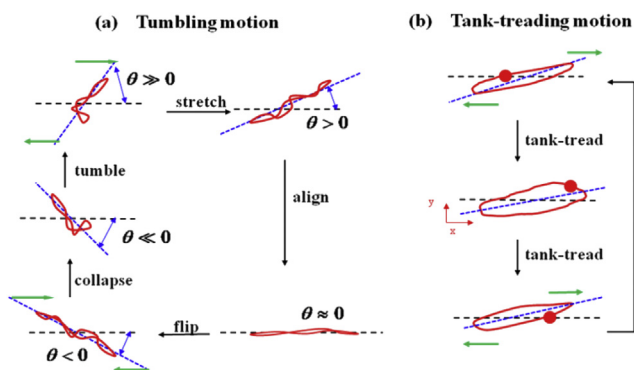


Fig. 8. Description the tumbling (a) and tank-treading (b) mechanisms of individual flexible ring polymers in simple shear flow.

where \mathbf{R}_i is the position vector of the bead i respect to the center of mass of the polymer chain and \mathbf{f}_i is the total force on bead i . The dimensionless shear viscosity is defined as

$$\eta = \frac{\tau_{xy}}{Wi} \quad (10)$$

Fig. 9 shows the shear evolution of the intrinsic viscosity relative to zero shear viscosity η_0 . There is a Newtonian plateau at low shear rate ($Wi \leq 1$). Then, with increasing Wi , the polymer solutions display nonlinear rheological behavior, where the flexible ring polymers begin to stretch and orient along the flow direction. The shear thinning behavior yields the scaling law $\eta \sim Wi^{-0.40}$ over the Wi range from 20 to 300. In addition, the polymer contribution to the shear viscosity η also scales linearly with G_{yy} in Giesekus expression for the stress tensor, so the scale -0.40 is nearly the same power law decay as exhibited by $G_{yy}^{-0.41}$, which is larger than the scale -0.5 of linear polymers [62].

The dimensionless first normal stress coefficient is calculated as

$$\psi_1 = \frac{\tau_{xx} - \tau_{yy}}{Wi^2} \quad (11)$$

In Fig. 10, the ring polymer contribution to the first normal stress coefficient ψ_1 is shown as a function of Wi . The first normal stress coefficient ψ_1 yields a power law $\psi_1 \sim Wi^{-0.90}$, while the linear polymers have a slightly stronger shear rate dependence $\psi_1 \sim Wi^{-1.23}$ [62]. The different scalings are expected according to a continuous stretching of the flexible ring chains in tank-treading motion.

4. Conclusions

In this work, the flow-induced behaviors of single flexible ring polymers in simple shear flow are studied by the multiparticle collision dynamics combined with molecular dynamics simulations. The conformational, orientational, dynamical and rheological properties of single flexible ring polymers with different chain lengths are analyzed in detail. Our results reveal that, consistent with linear polymers, the stretching of ring polymers in flow direction is accompanied by the compression in gradient and vorticity direction. The scaling behaviors show that ring polymers undergo weaker deformation and orientation than their linear analogues in the gradient direction, which is attributed to the continuous stretching and constant alignment in the tank-treading motion, while the tank-treading motion has no obvious influence on the flow-induced behaviors in the vorticity direction. Correspondingly, the rheological behaviors have a weak dependence on shear rate. In addition, we propose a general description model of

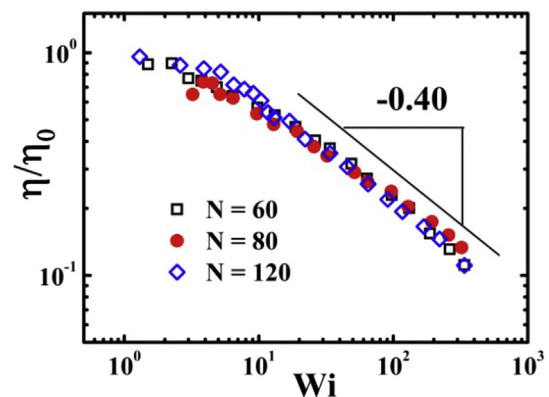


Fig. 9. Polymer contribution to shear viscosity η .

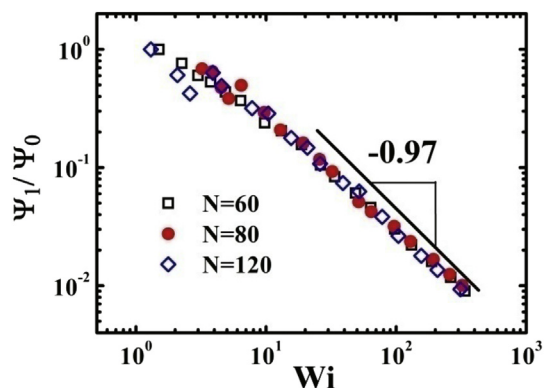


Fig. 10. Polymer contribution to the first normal stress coefficient Ψ_1 .

tumbling and tank-treading mechanisms in strong shear flow on the basis of the time trajectories of the relative deformation and orientation. When the plane of the stretched ring coincides with the shear plane, the velocity gradient causes the flexible ring polymers to perform a tank-treading motion, while rings undergo stretching and collapsing in the tumbling motion to avoid large shear gradient. The effects of two types of motions on the alignment of ring polymers are reflected in the scaling behavior of the orientational angle $\tan(2\theta)$ and the half-height width of the probability distribution functions.

Our simulations reveal the effect of the strong constraints without ends for ring polymers on conformational, orientational, dynamical and rheological properties and present the similarities and differences in the non-equilibrium behavior of ring and linear polymers. It has been well-known that these flow-induced behaviors play an important role in separation process and polymer physics, and the findings may therefore shed some light on cyclic DNA manufacturing and provide help for experiments.

Acknowledgement

This work was supported by National Natural Science Foundation of China (21274153, 21334007 and 21404105) and One Hundred Person Project of the Chinese Academy of Sciences. We are grateful to Computing Center of Jilin Province for essential support.

References

- [1] Semlyen JA. *Cyclic polymers*. 2nd ed. Dordrecht: Kluwer Academic Publishers; 2001.
- [2] Trabi M, Craik DJ. *Trends Biochem Sci* 2002;27:132.
- [3] Sanchez T, Kulic IM, Dogic Z. *Phys Rev Lett* 2010;104:098103.
- [4] Micheletti C, Orlandini E. *Macromolecules* 2012;45:2113.
- [5] Alberts B, Johnson A, Lewis J, Ra M, Roberts K, Walter P. *Molecular biology of the cell*. 4th ed. New York: Garland Science; 2002.
- [6] Drube F, Alim K, Witz G, Dietler G, Frey E. *Nano Lett* 2010;10:1445.
- [7] Tezuka Y. In: *Topological polymer chemistry: progress of cyclic polymers in syntheses, properties, and functions*. Singapore: World Scientific; 2013.
- [8] Shaqfeh ESG. *J Newt Fluid Mech* 2005;130:1.
- [9] Tegenfeldt JO, Prinz C, Cao H, Huang RL, Austin RH, Chou SY, et al. *Anal Bioanal Chem* 2004;378:1678.
- [10] Sheng JF, Luo KF. *Phys Rev E* 2012;86:031803.
- [11] de Gennes PG. *J Chem Phys* 1974;60:5030.
- [12] Larson RG, Magda JJ. *Macromolecules* 1989;22:3004.
- [13] Winkler RG. *Phys Rev Lett* 2006;97:128301.
- [14] Hinczewski M, Netz RR. *Macromolecules* 2011;44:6972.
- [15] Smith DE, Babcock HP, Chu S. *Science* 1999;283:1724.
- [16] LeDuc P, Haber C, Bao G, Wirtz D. *Nature* 1999;399:564.
- [17] Schroeder CM, Teixeira RE, Shaqfeh ESG, Chu S. *Phys Rev Lett* 2005;95:018301.
- [18] Delgado-Buscalioni R. *Phys Rev Lett* 2006;96:088303.
- [19] Gerashchenko S, Steinberg V. *Phys Rev Lett* 2006;96:038304.
- [20] Liu S, Ashok B, Muthukumar M. *Polymer* 2004;45:1383.
- [21] Tan S. *Polymer* 1999;40:695.
- [22] Khare R, Graham MD, de Pablo JJ. *Phys Rev Lett* 2006;96:224505.
- [23] Dalal IS, Albaugh A, Hoda N, Larson RG. *Macromolecules* 2012;45:9493.
- [24] Aust C, Hess S, Kroger M. *Macromolecules* 2002;35:8621.
- [25] Link A, Springer J. *Macromolecules* 1993;26:464.
- [26] Lee EC, Muller SJ. *Polymer* 1999;40:2510.
- [27] Teixeira RE, Babcock HP, Shaqfeh ESG, Chu S. *Macromolecules* 2005;38:581.
- [28] Hur JS, Shaqfeh ESG, Babcock HP, Chu S. *Phys Rev E* 2002;66:011915.
- [29] Dalal IS, Hoda N, Larson RG. *J Rheol* 2012;56:305.
- [30] Ghosh I, Joo YL, McKinley GH, Brown RA, Armstrong RC. *J Rheol* 2002;46:1057.
- [31] Doyle PS, Shaqfeh ESG, Gast AP. *J Fluid Mech* 1997;334:251.
- [32] Kahn DW, Butler MD, Cohen DL, Gordon M, Kahn JW, Winkler ME. *Biotechnol Bioeng* 2000;69:101.
- [33] Chang T. *Adv Polym Sci* 2003;163:1.
- [34] Lepoittevin B, Dourges MA, Masure M, Hemery P, Baran K, Cramail H. *Macromolecules* 2000;33:8218.
- [35] Roovers J. *Macromolecules* 1988;21:1517.
- [36] Zheng JJ, Yeung ES. *Anal Chem* 2003;75:3675.
- [37] Cifre JGH, Pamiés R, Martínez MCL, de la Torre JG. *Polymer* 2005;46:267.
- [38] Chen WD, Chen JZ, An LJ. *Soft Matter* 2013;9:4312.
- [39] Chen WD, Chen JZ, Liu LJ, Xu XL, An LJ. *Macromolecules* 2013;46:7542.
- [40] Lang PS, Obermayer B, Frey E. *Phys Rev E* 2014;89:022606.
- [41] Kapral R. *Adv Chem Phys* 2008;140:89.
- [42] Kroger M. *Phys Rep* 2004;390:453.
- [43] Malevanets A, Kapral R. *J Chem Phys* 1999;110:8605.
- [44] Malevanets A, Kapral R. *J Chem Phys* 2000;112:7260.
- [45] Nikoubashman A, Likos CN. *Macromolecules* 2010;43:1610.
- [46] Winkler RG, Huang CC. *J Chem Phys* 2009;130:074907.
- [47] Petersen MK, Lechman JB, Plimpton SJ, Grest GS, in't Veld PJ, Schunk PR. *J Chem Phys* 2010;132:174106.
- [48] Ji SC, Jiang R, Winkler RG, Gompper G. *J Chem Phys* 2011;135:104902.
- [49] Kowalik B, Winkler RG. *J Chem Phys* 2013;138:104903.
- [50] Wen XH, Zhang D, Zhang LX. *Polymer* 2012;53:873.
- [51] Allen MP, Tildesley DJ. *Computer simulation of liquids*. New York: Oxford University Press; 1987.
- [52] Doi M, Edwards SF. *The theory of polymer dynamics*. New York: Oxford University Press; 1986.
- [53] Ripoll M, Mussawisade K, Winkler RG, Gompper G. *Phys Rev E* 2005;72:016701.
- [54] Ihle T, Kroll DM. *Phys Rev E* 2001;63:020201.
- [55] Rapaport DC. *The art of molecular dynamics simulation*. New York: Cambridge University Press; 2004.
- [56] Huang CC, Chatterji A, Sutmann G, Gompper G, Winkler RG. *J Comput Phys* 2010;229:168.
- [57] Ripoll M, Mussawisade K, Winkler RG, Gompper G. *Europhys Lett* 2004;68:106.
- [58] Gompper G, Ihle T, Kroll DM, Winkler RG. *Adv Comput Simul Approaches Soft Matter Sci III* 2009;221:1.
- [59] Lu WY, Hu YH, Yang SH. *J Chem Phys* 1998;108:4705.
- [60] Huang CC, Winkler RG, Sutmann G, Gompper G. *Macromolecules* 2010;43:10107.
- [61] Winkler RG. *J Chem Phys* 2010;133:164905.
- [62] Schroeder CM, Teixeira RE, Shaqfeh ESG, Chu S. *Macromolecules* 2005;38:1967.
- [63] Fuller GG. *Optical rheometry of complex fluids*. New York: Oxford Univ. Press; 1995.
- [64] Bossart J, Öttinger HC. *Macromolecules* 1995;28:5852.
- [65] Tsvetkov NV, Lebedeva EV, Lezov AA, Podseval'nikova AN, Akhmadeeva LI, Zorin IM, et al. *Polymer* 2014;55:1716.
- [66] Cao Z, Zhang G. *Polymer* 2014;55:6789.
- [67] Chertkov M, Kolokolov I, Lebedev V, Turitsyn K. *J Fluid Mech* 2005;531:251.
- [68] Puliafito A, Turitsyn K. *Phys D* 2005;211:9.
- [69] Pivkin IV, Karniadakis GE. *Phys Rev Lett* 2008;101:118105.
- [70] Abkarian M, Favre M, Viallat A. *Phys Rev Lett* 2007;98:188302.
- [71] Bird RB, Hassager O, Armstrong RC, Curtiss CF. *Dynamics of polymeric liquids*. 2nd ed. New York: John Wiley & Sons; 1987.